

Intrinsic suppression of the topological thermal Hall effect in an exactly solvable quantum magnetS. Suetsugu ¹, T. Yokoi,¹ K. Totsuka,² T. Ono,¹ I. Tanaka,¹ S. Kasahara ^{1,3}, Y. Kasahara,¹
Z. Chengchao ⁴, H. Kageyama,⁴ and Y. Matsuda¹¹*Department of Physics, Kyoto University, Kyoto 606-8502, Japan*²*Yukawa Institute for Theoretical Physics, Kyoto University, Kyoto 606-8502, Japan*³*Research Institute for Interdisciplinary Science, Okayama University, Okayama 700-8530, Japan*⁴*Department of Energy and Hydrocarbon Chemistry, Kyoto University, Nishikyo-ku, Kyoto 615-8510, Japan*

(Received 20 July 2021; accepted 4 January 2022; published 14 January 2022)

In contrast to electron (fermion) systems, topological phases of charge neutral bosons have been poorly understood despite recent extensive research on insulating magnets. The most important unresolved issue is how the inevitable interbosonic interactions influence the topological properties. It has been proposed that the quantum magnet $\text{SrCu}_2(\text{BO}_3)_2$ with an exact ground state serves as an ideal platform for this investigation, as the system is expected to be a magnetic analog of a Chern insulator with electrons replaced by bosonic magnetic excitations (triplons). Here, in order to examine topologically protected triplon chiral edge modes in $\text{SrCu}_2(\text{BO}_3)_2$, we measured and calculated the thermal Hall conductivity κ_{xy} . Our calculations show that the sign of κ_{xy} is negative, which is opposite to the previous calculations, and its magnitude is 2π times smaller. No discernible κ_{xy} was observed, and its values are at most 20–30% of our calculations if present. This implies that even relatively weak interparticle interactions seriously influence the topological transport properties at finite temperatures. These findings demonstrate that, in contrast to fermionic cases, the picture of noninteracting topological quasiparticles cannot be naively applied to bosonic systems, calling special attention to the interpretation of the topological bosonic excitations reported for various insulating magnets.

DOI: [10.1103/PhysRevB.105.024415](https://doi.org/10.1103/PhysRevB.105.024415)**I. INTRODUCTION**

The discoveries of electronic topological materials having gapped bulk excitations and topologically protected gapless edge states have led to a quest for similar effects in systems with quasiparticles obeying different quantum statistics. In the past few years, quantum insulating magnets with Dzyaloshinskii-Moriya (DM) interaction have attracted renewed interest because they have raised the prospect of harboring topologically protected edge states of bosonic spin excitations [1–3] (for recent developments, see, e.g., Ref. [4] and the references cited therein). As these excitations are charge neutral, they do not respond to an electromagnetic field but can carry heat and potentially exhibit the thermal Hall effect [5,6] without resorting to the Lorentz force. Recently, finite thermal Hall conductivity κ_{xy} has been experimentally resolved in several insulating magnets on geometrically frustrated lattices [7–13], which has been interpreted as the predicted topological thermal Hall effect of bosonic spin excitations. These topological excitations have gained great interest as they have the potential to realize dissipationless spintronic or magnonic devices [14].

However, the validity of the conclusion concerning the topological chiral edge current of bosonic particles should be scrutinized because several important issues remain unresolved. For instance, it has been shown theoretically that in frustrated ferromagnets, finite cubic interactions among bosons may yield nonperturbative damping of magnon modes even at $T = 0$ [15]. This can dramatically alter the existing

picture based on stable bosonic quasiparticles with topologically nontrivial properties, in contrast to the fermionic counterpart where particle-number conservation forbids such cubic interactions from appearing. In addition, quantitative comparison of the observed thermal Hall effect with theory is difficult and often impossible in most frustrated quantum magnets, because their ground states and low-energy excitations are not fully understood. Furthermore, recent studies on insulating magnets such as kagome antiferromagnets with weak lattice-spin coupling revealed the presence of a non-negligible contribution of the thermal Hall effect of phononic origin [13,16–18], which makes it difficult to single out the topological part. In fact, the thermal Hall conductivity κ_{xy} observed in the frustrated pyrochlore ferromagnet $\text{Lu}_2\text{V}_2\text{O}_7$, which contains a two-dimensional (2D) kagome lattice, is much larger than that expected from the DM interaction determined by density functional theory [19,20], indicating that the observed κ_{xy} may not be solely of topological origin. Given these facts, it is safe to say that the topological chiral edge current of bosonic spin excitations, including its presence, remains largely unexplored. To investigate the elusive nontrivial bosonic topology, knowledge of the thermal Hall effect of topological bosons in magnetic systems with exactly solvable ground states, in which precise comparison between theory and experiments is possible, is crucially important.

A candidate material that appears to be most suitable for such an investigation is $\text{SrCu}_2(\text{BO}_3)_2$ [21], a frustrated layered quantum spin system. Each layer of this material consists of a 2D network of orthogonal dimers of spin-1/2

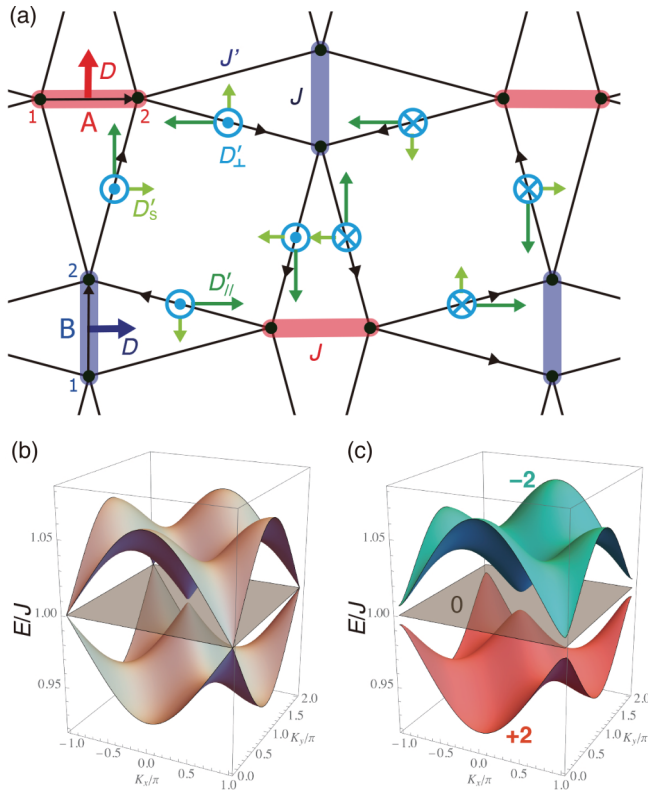


FIG. 1. Basic properties of $\text{SrCu}_2(\text{BO}_3)_2$. (a) Shastry-Sutherland lattice and DM interactions in $\text{SrCu}_2(\text{BO}_3)_2$. The thick red and blue lines represent the two species of dimers (A and B) of spin-1/2 Cu^{2+} ions. The black arrows ($i \rightarrow j$) indicate the order of the spins \mathbf{S}_i and \mathbf{S}_j in the DM interactions $\mathbf{D}_{ij} \cdot (\mathbf{S}_i \times \mathbf{S}_j)$ on the bond (i, j). The intradimer DM interaction has only an in-plane component (red and blue arrows). For interdimer interactions, all three components are allowed by symmetry. (b) and (c) Triplon bands of $\text{SrCu}_2(\text{BO}_3)_2$ at zero (b) and small magnetic field (c). The triplon bands at zero field form a Dirac cone with three bands (two dispersive bands and one flat band) touching at the M point. A small magnetic field opens the band gap, yielding the two separated bands with nontrivial Chern numbers ± 2 as well as a trivial one.

Cu^{2+} ions [see Fig. 1(a)]. The magnetic properties are well described by the 2D Heisenberg model with antiferromagnetic (AFM) nearest-neighbor (intradimer) and AFM next-nearest-neighbor (interdimer) exchange couplings, J and J' , known as the Shastry-Sutherland model [22]. It has been shown that for $J'/J \leq 0.675$, an unentangled product of dimer singlets is the exact ground state [23], and $\text{SrCu}_2(\text{BO}_3)_2$ with $J'/J \approx 0.63$ is believed to be in this phase [24].

The first excited state, separated from the ground state by a finite spin gap of ~ 3 meV, is a bosonic $S = 1$ quasiparticle dubbed a *triplon*, which corresponds to exciting one of the dimer singlets to a triplet [25]. Without any additional interactions, the three triplon bands are triply degenerate and have very tiny dispersion of the order of $(J'/J)^6 \sim 6 \times 10^{-2}$ [26]. Note that this extremely small band width is attributed not to the smallness of the interdimer interaction J' but to the unique orthogonal-dimer structure [see Fig. 1(a)], and the triplons in $\text{SrCu}_2(\text{BO}_3)_2$ are essentially strongly interacting as is exemplified by, e.g., its magnetic bound states and the unique magnetization process [24,27].

Below a structural transition temperature $T_s \sim 395$ K, the dimer plane is slightly buckled. As a result, DM interactions are allowed by symmetry both on each dimer and between neighboring dimers [28,29], as illustrated in Fig. 1(a). The known experimental values are $J = 3.08$ meV and $D'_\perp = -0.097$ meV [30]. In the presence of the small but finite DM interactions, the triply degenerate and dispersionless triplon band is modified, resulting in three subbands with weak dispersion (of the order of the DM interactions) as observed in inelastic neutron scattering [30–32] and electron spin resonance (ESR) experiments [33].

It has been proposed theoretically that the perpendicular component D'_\perp of the interdimer DM interactions endows the triplon bands with a topological character [30,34–36] and turns the system into a magnetic analog of the Chern insulators. Without the external magnetic field perpendicular to the dimer plane, the triplons form a Dirac cone with three bands touching at a single point (the M point) as seen in Fig. 1(b). A small magnetic field opens a band gap at the Dirac point, leading to two topological bands with the Chern numbers ± 2 [Fig. 1(c)]. As a result, the stable triplons moving under the momentum-space Berry flux, which is determined by the triplon band structure, are expected to show the thermal Hall effect. As will be discussed later, the geometrically suppressed kinetic energy of triplons in $\text{SrCu}_2(\text{BO}_3)_2$ prevents their spontaneous decay at $T = 0$ [15,37] that may potentially invalidate the picture based on topologically nontrivial quasiparticles. Therefore this system seems to provide a unique playground to study the topological properties of bosonic quasiparticles.

Here, we report the results of high-resolution thermal Hall conductivity κ_{xy} measurements on the exactly solvable quantum magnet $\text{SrCu}_2(\text{BO}_3)_2$. In contrast to the theoretical predictions, we observed no discernible κ_{xy} within our experimental resolution. The strong suppression of κ_{xy} implies that topological transport phenomena are strongly influenced by the interparticle interactions in bosonic systems.

II. METHODS

Single crystals of $\text{SrCu}_2(\text{BO}_3)_2$ were grown by a traveling-solvent floating-zone method. The crystal was polished into a platelike shape of roughly $1.5 \times 0.46 \times 0.025$ mm for thermal transport measurements. Four gold wires were attached by silver paste to serve heat links to a 1-k Ω chip as a heater and three Cernox (CX1070) thermometers as seen in the inset to Fig. 2. One end of the crystal was glued to a LiF heat bath using nonmetallic grease. Thermal and thermal Hall conductivities were measured simultaneously by a standard steady-state method by applying temperature gradient j and magnetic field H along the crystallographic a and c axis, respectively. To exclude the contribution from misalignment of the contacts, antisymmetric components of the measured $\nabla_y T$ were numerically calculated and used to obtain $\kappa_{xy}(H)$.

III. RESULTS

Figure 2 depicts the temperature dependence of longitudinal thermal conductivity κ_{xx} in zero field. As the temperature is lowered, κ_{xx} decreases gradually and then increases below 10 K forming a peak at around 4 K. The magnitude of κ_{xx} at the peak in the present crystal, which reflects the quality of

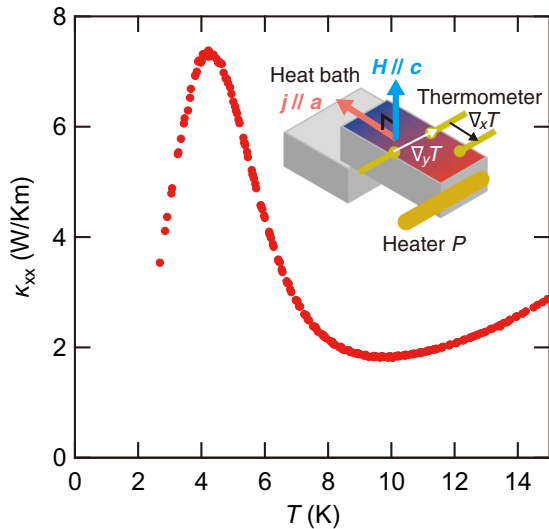


FIG. 2. Temperature dependence of thermal conductivity κ_{xx} of $\text{SrCu}_2(\text{BO}_3)_2$ at zero field. The inset shows the experimental setup for thermal and thermal Hall conductivity measurements.

the crystal, is close to the highest value reported so far [38], indicating the high quality of our crystal.

We first discuss the behaviors of the thermal Hall effect predicted theoretically. The solid and dashed curves in Figs. 3(a) and 3(b) represent the field dependence of κ_{xy} calculated for $T = 7, 8.5,$ and 10 K by the formula equation (B1) [39], which assumes stable noninteracting triplon excitations subject to the Berry curvature (see Appendixes A and B for more information). We note that the topological thermal Hall effect is absent at zero temperature and appears only at finite temperatures where the triplon bands with non-trivial Chern numbers are thermally populated. Its magnitude depends not only on the Berry curvature $F_{xy}^{(m)}(\mathbf{K})$ of the topological bands but also on how these bands are occupied by thermally excited triplons [5,6]. Finite κ_{xy} , which is negative in sign, appears at weak magnetic fields. At around $\mu_0 H \approx$

0.7 T, the absolute value of κ_{xy} shows a maximum and then decreases with H . Above a threshold field of $\mu_0 H_{\text{th}} \approx 1.5$ T, which is set by the out-of-plane component D_{\perp} , the Chern number changes from ± 2 to zero (see Appendix A 2), and the triplon bands lose their topological character, resulting in a rapid decrease in κ_{xy} . Unlike the Hall conductance in fermionic band insulators, where the topological bands are occupied homogeneously in k space at $T = 0$, the thermal Hall conductivity is not quantized in the present bosonic system; being the integral of the local Berry curvature and the thermal occupation factor [see Eq. (B1)], its value depends crucially on the detailed structure of the quasiparticle bands and is not at all universal. This is why the values of κ_{xy} are very different in magnitude depending on the systems [7,11]. In fact, even after the Chern number vanishes, small but finite κ_{xy} survives due to the nonvanishing (local) Berry curvature.

In stark contrast to the theoretical predictions [34], however, no discernible thermal Hall signal is detected within our experimental resolution, as shown by the red circles in Fig. 3(a) and the green hexagons and the blue squares in Fig. 3(b). The observed κ_{xy} at $T = 7, 8.5,$ and 10 K is at most 20–30% of the theoretical values, if present. We also checked that this substantial discrepancy between the theoretical and experimental values is not accidental [40].

Prior to our results, it has also been reported [41] that κ_{xy} is smaller than the theoretical prediction. However, due to the large error bars of the measurements, there have been no conclusive data for the magnitude of κ_{xy} so far. Here, our ability to control the temperature very precisely, $\delta T \sim 50 \mu\text{K}$ ($\delta T/T \sim 10^{-5}$; see Appendix C), enables us to achieve high-precision measurements of κ_{xy} , whose resolution is significantly improved from the previous report.

IV. DISCUSSION

The present results lead us to conclude that the thermal Hall effect of topological origin predicted theoretically [34] is absent in $\text{SrCu}_2(\text{BO}_3)_2$. In this section, we examine several possible reasons for this large discrepancy between the

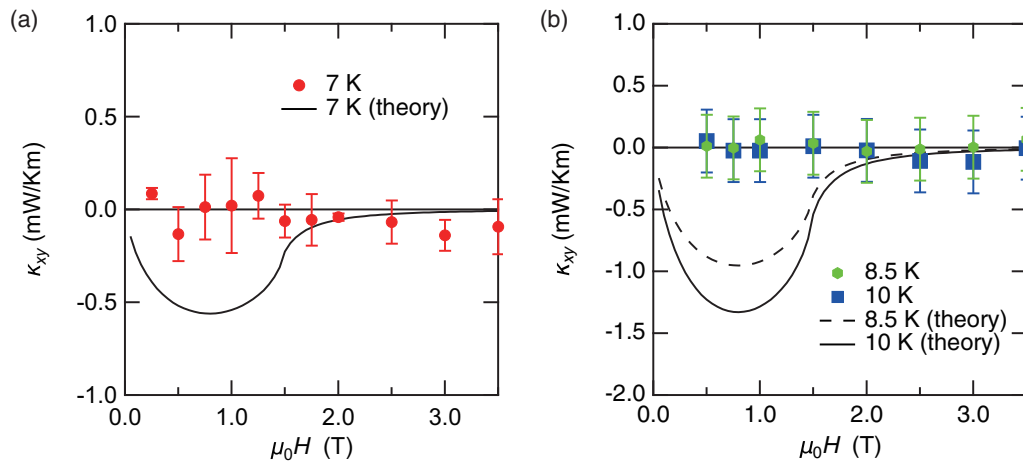


FIG. 3. Field dependence of thermal Hall conductivity κ_{xy} of $\text{SrCu}_2(\text{BO}_3)_2$. (a) and (b) The observed κ_{xy} at 7, 8.5, and 10 K (red, green, and blue symbols), and the calculated κ_{xy} at 7, 8.5, and 10 K (solid and dashed curves). No discernible κ_{xy} was detected within our experimental resolution. The error bars in the 7-K data represent a standard statistical error (see Appendix C for details). The error bars for the 8.5- and 10-K data were estimated from the largest error bar of the 7-K data.

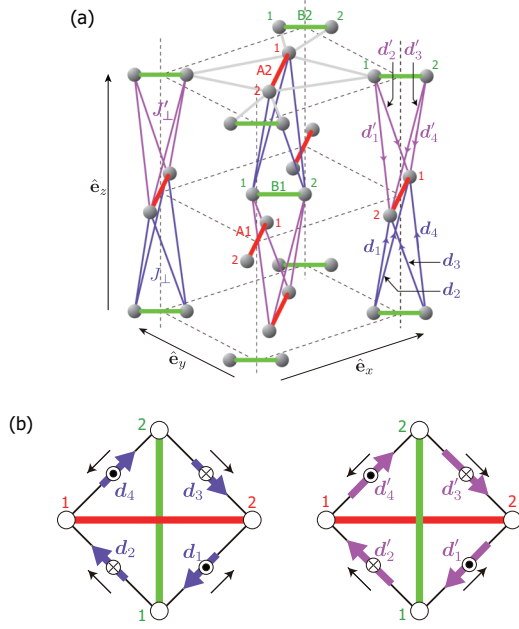


FIG. 4. Three-dimensional structure of SrCu₂(BO₃)₂ and symmetry-allowed interlayer DM interactions (a), and its top view (b). Due to the buckling in the *ab* plane, the interlayer DM interactions can be different for A-B [left panel of (b); $d_{y,z}$] and B-A [right panel of (b); $d'_{y,z}$] pairs.

theoretical prediction based on the picture of stable noninteracting quasiparticles and the experimental results.

A. Domain formation

We begin by considering a few extrinsic sources of the strong suppression of κ_{xy} . First of all, the sample is expected to contain structural domains with different patterns of buckling in the *ab* plane. The buckling is crucial for the nonzero thermal Hall response as it induces the in-plane component D'_{\parallel} of the DM interactions [29] which is necessary for the finite Berry curvature [see Eq. (A5)]. However, the absence of the thermal Hall effect cannot be attributed to the domain formation for the following reason. To be specific, we assume that the A (B) dimers are shifted upward (downward) from the basal planes. Then, in a system where the directions of the shift are reversed, all the *in-plane* components of the DM interactions (i.e., D , D'_s , and D'_{\parallel}) are flipped. However, since both the triplon dispersion (A4) and the Berry curvature (A5) depend only on $D'_{\parallel}{}^2$ [42], κ_{xy} from different domains have the same sign and do not cancel each other.

B. Effects of interlayer couplings

The interactions among the Shastry-Sutherland layers may affect the thermal Hall conductivity (B1) calculated for the purely two-dimensional system. In the actual SrCu₂(BO₃)₂ compound, there are several kinds of interlayer interactions that might modify the 2D physics. First of all, there are exchange couplings of the following form on the shortest bonds connecting the adjacent layers [24]:

$$J_{\perp}(\mathbf{S}_{A,1} + \mathbf{S}_{A,2}) \cdot (\mathbf{S}_{B,1} + \mathbf{S}_{B,2}) = J_{\perp} \mathbf{T}_A \cdot \mathbf{T}_B, \quad (1)$$

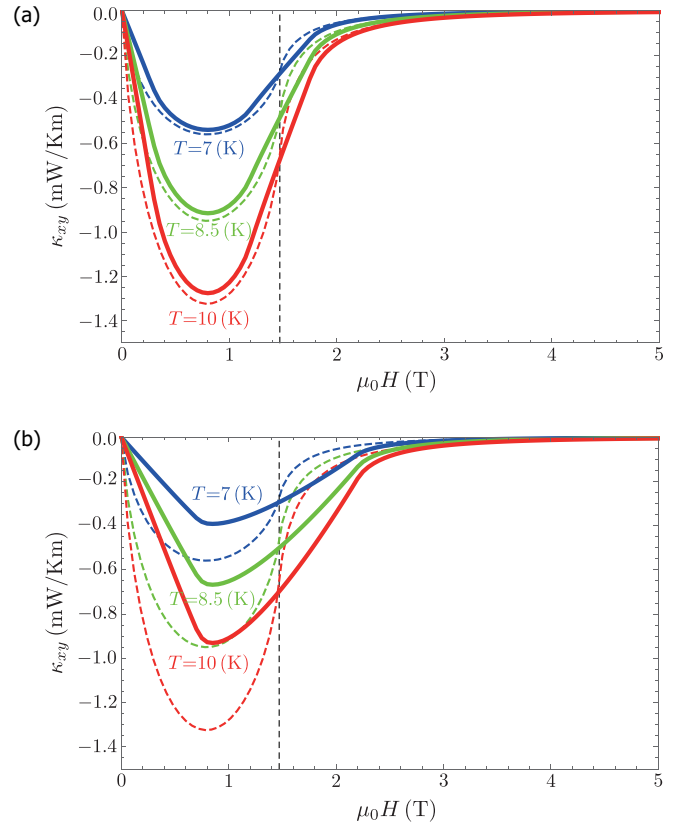


FIG. 5. Thermal Hall conductivity $\kappa_{xy}^{3D}(T, H_z)$ (solid curves) and its 2D limit $\kappa_{xy}(T, H_z)$ (dashed curves) for different temperatures. The interlayer DM interactions are assumed to be (a) $d_z = 0.2D'_{\perp}$ or (b) $d_z = 0.5D'_{\perp}$. At $\mu_0 H = 1.47$ T (dashed line), a band-touching transition occurs, and the triplon bands lose their topological character.

where the A and B dimers are on the upper and lower layers, respectively, or vice versa. As this interaction vanishes when at least one of A and B is occupied by a singlet, it does not help a singlet triplon to hop between adjacent layers [43]. This conclusion remains the same even when many triplons exist. If we note that the J_{\perp} interaction itself does not change the positions of triplons, we see that the interlayer interaction J_{\perp} does not contribute to any kind of triplon motion at all.

On top of the usual exchange couplings, the crystal symmetry allows several DM interactions between layers as shown in Fig. 4. It is also suggested [44] that the interlayer DM interactions allowed by symmetry can change the topological properties of an isolated plane. We calculated the triplon spectrum and the thermal Hall conductivity in the presence of such interlayer DM interactions:

$$\kappa_{xy}^{3D}(T, H_z) = \frac{1}{\pi} \int_{H_z - \frac{2|d_z|}{g_z \mu_B}}^{H_z + \frac{2|d_z|}{g_z \mu_B}} \frac{\kappa_{xy}(T, h)}{\sqrt{\left(\frac{2d_z}{g_z \mu_B}\right)^2 - (h - H_z)^2}} dh \quad (2)$$

(see Appendix B 2 for the derivation). In deriving the above formula, we have assumed, for simplicity, that the z components of the eight interlayer DM interactions have a common absolute value d_z . We plot $\kappa_{xy}^{3D}(T, H_z)$ calculated by Eq. (2) in Fig. 5 for two different values of the interlayer DM interaction d_z . No precise information is available on the values of the

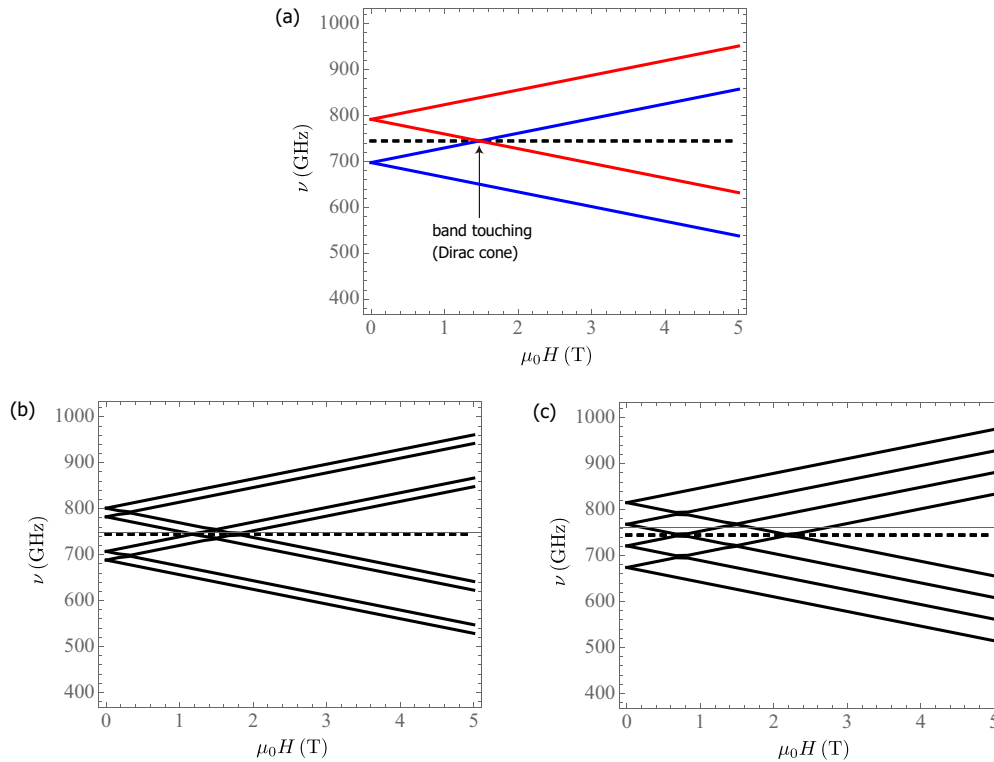


FIG. 6. Energy levels at the Γ point which are to be compared with the ESR spectrum in, e.g., Ref. [33]: for (a) $d_z = 0$, (b) $d_z = 0.2D'_\perp$, and (c) $d_z = 0.5D'_\perp$. At the level crossing at $\mu_0 H = 1.47$ T (a), the triplon bands lose their topological properties. The six levels for $d_z = 0$ are further split by interlayer DM interactions d_z .

interlayer DM interactions in $\text{SrCu}_2(\text{BO}_3)_2$ for now; we can obtain a crude estimate of d_z by comparing the theoretical spectrum with the ESR results [33]. We plot in Fig. 6 the spectrum of the interlayer DM interactions d_z which are compatible with the ESR results [33] do not reduce κ_{xy} substantially.

C. Magnetophonon coupling

A magnetophonon coupling, which has been pointed out by a resonant scattering observed in the longitudinal thermal conductivity measurements [38], can be an origin of the triplon damping. However, because the magnetophonon coupling is most active around 20 K, such a coupling is unlikely to be an origin of the strong suppression of the thermal Hall conductivity at lower temperatures (e.g., 7–10 K). Indeed, a correlated decay process of the triplon excitations which is responsible for the triplon damping at $T \leq 10$ K [32] cannot be explained solely by acoustic phonons.

D. Triplon-triplon interaction

Having excluded the extrinsic sources of the suppression, one may ask about the stability of triplon quasiparticles against additional interactions which have not been included in the previous analyses [30,34]. The realization of topological magnon bands in other spin systems has been proposed for the frustrated kagome ferromagnets, such as $\text{Lu}_2\text{V}_2\text{O}_7$ [7,8] and $\text{Cu}[1,3\text{-benzenedicarboxylate (bdc)}]$ [3]. It has been shown theoretically that in these systems the DM interactions

not only provide the quasiparticles with nontrivial topological characters, but also generate anharmonic (e.g., cubic) interactions among them leading to their damping [15]. To be specific, we here consider the anharmonic cubic coupling of the form $b^\dagger b^\dagger b$ [with b^\dagger (b) being the bosonic creation (annihilation) operator for triplons or magnons], which has been discussed as an origin of the magnon damping [37]. Such a cubic interaction leads to the decay of a single bosonic quasiparticle (with energy $\epsilon_{\mathbf{k}}$) into two, satisfying the conservation of energy and momentum: $\epsilon_{\mathbf{k}} = \epsilon_{\mathbf{q}} + \epsilon_{\mathbf{k}-\mathbf{q}}$. For this constraint to be satisfied in the decay process, an overlap between the two-particle continuum and a single-particle band is required, as illustrated in Fig. 7(a). In the above kagome ferromagnets with such an overlap, cubic interactions induced by DM interactions in fact lead to strong decay of topological magnons even at $T = 0$, as pointed out in Ref. [15].

It is known that such a cubic interaction $b^\dagger b^\dagger b$ (of the order of J') exists in $\text{SrCu}_2(\text{BO}_3)_2$ already in the absence of the DM interactions [45]. However, it should be stressed that, in stark contrast to the magnons with sizable dispersions of the order of the exchange interactions found in the above frustrated magnets, the prerequisite overlap is absent in the triplons in $\text{SrCu}_2(\text{BO}_3)_2$. In fact, as shown in Fig. 7(b), the triplon bandwidth (~ 0.5 meV) is substantially suppressed in comparison to the spin gap (~ 3 meV) due to the unique (i.e., orthogonal-dimer) lattice geometry of $\text{SrCu}_2(\text{BO}_3)_2$, and the two-triplon continuum is well separated from the single-triplon band [31]. Therefore this decay process is forbidden at $T = 0$, suggesting that the damping caused by the anharmonic couplings is expected to be much smaller if present.

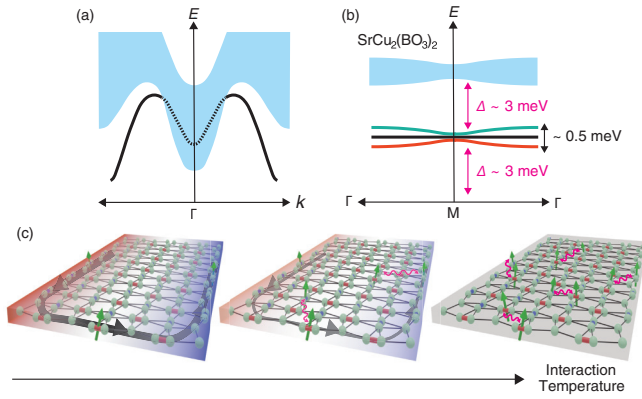


FIG. 7. Damping of bosonic spin excitations and destruction of topological properties. (a) Single-magnon band (solid curves) and two-magnon continuum (light blue area) in an $S = 1$ Heisenberg chain. The single-magnon band overlaps the two-magnon continuum around the Γ point, yielding the nonperturbative damping of magnons. (b) Single-triplon band (solid curves) and two-triplon continuum (light blue area) in $\text{SrCu}_2(\text{BO}_3)_2$. The spin gap $\Delta \sim 3$ meV, much larger than the triplon bandwidth of ~ 0.5 meV, avoids an overlap of the single-triplon band and two-triplon continuum, and therefore the spontaneous decay does not occur at 0 K. (c) Schematic illustration of the triplon edge current in the presence of interactions between thermally populated triplons in $\text{SrCu}_2(\text{BO}_3)_2$. The left panel displays the triplon edge current in the absence of the interaction. With increasing interaction and/or temperature, the topologically nontrivial properties are severely affected by the interaction between thermally excited bosons and are eventually almost destroyed, as illustrated in the middle and right panels.

Therefore we need to consider the effects of finite temperatures and the interaction among the thermally excited triplons, which has not been taken into account seriously in the previous calculations. One plausible origin for the strong suppression of κ_{xy} may be triplon damping at finite temperatures found in inelastic neutron scattering measurements [32]. However, the strong suppression of κ_{xy} cannot be simply understood by the quasiparticle damping alone for the following reason. Although the experiments observed a strong finite-temperature damping of the triplon excitations, the well-defined peak associated with a single-triplon excitation still remains below 10 K [32]. In particular, at $T = 7$ K, at which the thermal Hall measurements were done, a sharp single-triplon peak is observed, which means that a *single* triplon quasiparticle is stable at low enough temperatures. Therefore, as long as the picture based on *noninteracting* quasiparticles of topological character is correct, it is unlikely that the band broadening due to the damping has such a dramatic effect as to wipe out the thermal Hall signal almost completely. In this respect, the absence of κ_{xy} is surprising, implying that, in contrast to fermionic systems in which the noninteracting limit is well defined, topological transport phenomena in their bosonic counterparts are substantially influenced by small but finite particle-particle interactions.

V. SUMMARY AND OUTLOOK

In summary, we measured the thermal Hall conductivity of the exactly solvable quantum magnet $\text{SrCu}_2(\text{BO}_3)_2$ and

compared the results with the theoretical values calculated by assuming the existence of stable noninteracting quasiparticles (triplons). According to our calculations, the sign of κ_{xy} is negative, and the magnitude is reduced by a factor of 2π , as opposed to the previous theoretical predictions. The measurements were performed with extremely high accuracy, and we observed no discernible κ_{xy} , the values of which are at most 20–30% of our calculations if present. The strong suppression of κ_{xy} cannot be simply explained by the triplon damping at finite temperature, indicating that the interparticle interactions dramatically alter the topological transport properties. These arguments suggest that, in order to understand the thermal Hall transport in $\text{SrCu}_2(\text{BO}_3)_2$ even qualitatively, it is crucially important to take into account the strong interactions among a macroscopic number of thermally excited triplons [see Fig. 7(c)], which requires further theoretical investigations. Higher-order interactions between bosonic particles, which have never been considered in the topological context, may be an origin for the disappearance of the topological thermal Hall effect. The present study also calls special attention to the existing interpretation of the thermal Hall effect observed in various insulating magnets in terms of topological bosonic excitations.

ACKNOWLEDGMENTS

We thank Karlo Penc, Judit Romhányi, and Mike Zhitomirsky for insightful discussions. This work is supported by Grants-in-Aid for Scientific Research (KAKENHI) (No. JP18H01177, No. JP18H01180, No. JP18H05227, No. JP21H04443, and No. 21K13881) and Grant-in-Aid for Scientific Research on Innovative Areas (KAKENHI) “Quantum Liquid Crystals” (No. 19H05824) from the Japan Society for the Promotion of Science, and JST CREST (JPMJCR19T5).

APPENDIX A: TRIPLONS IN AN ORTHOGONAL-DIMER SYSTEM

1. Ground state and low-lying excitations

It is well known that the basic properties of $\text{SrCu}_2(\text{BO}_3)_2$ (SCBO) below a structural transition at $T_s \sim 395$ K are well described by the Shastry-Sutherland model [22] with the DM interactions added [28,29] [see Fig. 1(a)]:

$$\begin{aligned} \mathcal{H}_{\text{SCBO}} = & J \sum_{\text{n.n.}} \mathbf{S}_i \cdot \mathbf{S}_j + J' \sum_{\text{n.n.n.}} \mathbf{S}_i \cdot \mathbf{S}_j - \mu_B \sum_i \mathbf{H}_g \cdot \mathbf{S}_i \\ & + \sum_{\text{n.n.}} \mathbf{D}_{ij} \cdot (\mathbf{S}_i \times \mathbf{S}_j) + \sum_{\text{n.n.n.}} \mathbf{D}'_{ij} \cdot (\mathbf{S}_i \times \mathbf{S}_j), \quad (\text{A1}) \end{aligned}$$

where $\sum_{\text{n.n.}}$ ($\sum_{\text{n.n.n.}}$) denotes the summation over nearest-neighbor (next-nearest-neighbor) spin pairs ($\mathbf{S}_i, \mathbf{S}_j$) and, to ease the notation, we have included the magnetic constant μ_0 in the definition of \mathbf{H} . In the absence of the DM interactions, the exact ground state for $J'/J \leq 0.675$ is given by putting spin singlets on all the dimer bonds. The low-lying excitation over the exact ground state is given by exciting one of the dimer singlets into a triplet (a *triplon*). The interdimer exchange interaction J' gives only an isolated triplon an extremely tiny dispersion $\sim (J'/J)^6 \sim 6 \times 10^{-2}$ [26] except for renormalizing the spin gap (or the effective dimer coupling J).

On the other hand, the DM interactions allowed by crystallographic symmetry provide the triplons with a larger bandwidth of the order of $\sim D'$. Therefore, as far as the (cubic and quartic) interactions can be neglected, it would be legitimate to consider the effective Hamiltonian in which only the hopping of the order of the DM interactions is kept and J is replaced with its renormalized value (i.e., the observed spin gap). The resulting triplon Hamiltonian (the kernel of the quadratic part of the triplon Hamiltonian, precisely) can be written in the following suggestive form [34]:

$$\mathcal{H}_{3\text{-band}}(\mathbf{K}_x, \mathbf{K}_y) = J\mathbb{I} + \mathbf{B}(\mathbf{K}_x, \mathbf{K}_y) \cdot \mathcal{T}, \quad (\text{A2})$$

with the three matrices

$$\mathcal{T}_x = \begin{pmatrix} 0 & 0 & 0 \\ 0 & 0 & -1 \\ 0 & -1 & 0 \end{pmatrix}, \quad \mathcal{T}_y = \begin{pmatrix} 0 & 0 & -1 \\ 0 & 0 & 0 \\ -1 & 0 & 0 \end{pmatrix},$$

$$\mathcal{T}_z = \begin{pmatrix} 0 & i & 0 \\ -i & 0 & 0 \\ 0 & 0 & 0 \end{pmatrix}$$

satisfying the usual spin commutation relations and the fictitious “magnetic field” \mathbf{B} defined by

$$\mathbf{B}(\mathbf{K}_x, \mathbf{K}_y) = (\bar{D}'_{\parallel} \sin K_y, \bar{D}'_{\parallel} \sin K_x, g_z \mu_B H - D'_{\perp} (\cos K_x + \cos K_y)). \quad (\text{A3})$$

Thanks to the simple form (A2), the three triplon bands are explicitly written down as

$$\epsilon^{(m)}(\mathbf{K}_x, \mathbf{K}_y) = J + m|\mathbf{B}(\mathbf{K}_x, \mathbf{K}_y)| \quad (m = -1, 0, 1). \quad (\text{A4})$$

When the external field perpendicular to the dimer plane is absent ($H = 0$), there are two Dirac cones with three bands touching at $(\mathbf{K}_x, \mathbf{K}_y) = (\pi, 0)$ and $(0, \pi)$ corresponding to the existence of the two inequivalent dimers (A and B) in a unit cell [Fig. 1(b)].

2. Topology of triplon bands

A small perpendicular magnetic field H opens a band gap ($\sim H$) at the Dirac point [Fig. 1(c)], leading to two topological bands (top and bottom) with the Chern numbers ± 2 and one trivial one in the middle. The perpendicular component D'_{\perp} of the interdimer DM interactions endows the triplon bands with a topological character [30,34–36] and turns the system into a magnetic analog of the Chern insulators. Specifically, the three split triplon bands ($m = -1, 0, 1$) have the following Berry curvatures in the momentum space [46]:

$$F_{xy}^{(m)}(\mathbf{K}_x, \mathbf{K}_y) = -\frac{m\{D'_{\perp}(\cos K_x + \cos K_y) - g_z \mu_B H \cos K_x \cos K_y\}}{|\mathbf{B}(\mathbf{K}_x, \mathbf{K}_y)|^3} \bar{D}'_{\parallel}{}^2. \quad (\text{A5})$$

As a result, the stable triplons moving under the K -space Berry curvature, which is determined by the triplon band structure, are expected to exhibit the thermal Hall effect [5,6]. The nontrivial topology of the triplon bands can be character-

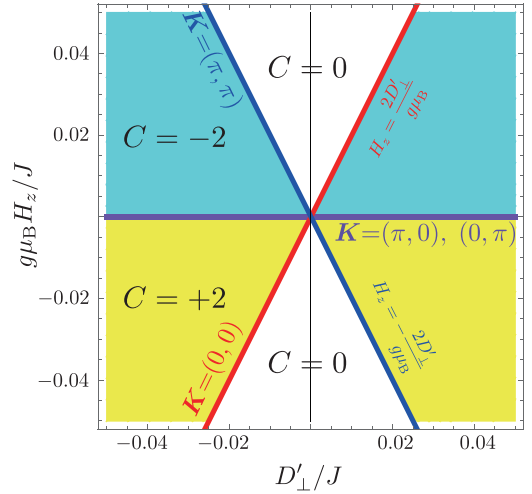


FIG. 8. Change in the triplon character in the (D'_{\perp}, H_z) plane. The Chern number $C^{(1)}$ of the top band (that of the bottom band is $-C^{(1)}$) and the positions of Dirac cones are shown. There are two topological “phases” with Chern number $C^{(1)} = +2$ (yellow) and $C^{(1)} = -2$ (cyan) as well as one trivial region ($C^{(1)} = 0$) at high fields that are separated from each other by band-touching transitions (thick lines) with Dirac cones (whose positions in \mathbf{K} space are shown).

ized by the Chern numbers defined by

$$C^{(m)} = \frac{1}{2\pi} \int_{\text{B.Z.}} d^2\mathbf{K} F_{xy}^{(m)}(\mathbf{K}_x, \mathbf{K}_y) \quad (m = -1, 0, 1) \quad (\text{A6})$$

(where B.Z. refers to the Brillouin zone), which, for a weak enough field, take the values $C^{(m)} = -2m$ [see Fig. 1(c)].

When the external field is further increased, another change in the band structure takes place at $|H_z| = |D'_{\perp}|/(2g\mu_B)$ accompanied by a band touching with a single Dirac cone at $\mathbf{K} = (\pi, \pi)$. When $|H_z| > |D'_{\perp}|/(2g\mu_B)$, $C^{(m)} = 0$ and the triplon bands lose their topological characters. The change in the topological character of the triplon bands is summarized in Fig. 8 as a function of the field H .

APPENDIX B: THERMAL HALL EFFECT FROM A TOPOLOGICAL TRIPLON

In the presence of finite Berry curvature, we may generically expect the Hall response in the electrical or thermal transport [47], and the general formula for the thermal Hall conductivity due to magnetic quasiparticles can be derived either by semiclassical arguments or by linear response theory [6].

1. Limit of uncoupled layers

When the two-dimensional Shastry-Sutherland layers (with the linear sizes $L_x \times L_y \times L_z$ and the number of layers N_{layer}) are not coupled with each other, the general formula given in Ref. [6] leads us to the following result [34]:

$$\kappa_{xy}(T, H) = -\frac{k_B^2 T}{2\pi h l_z} \int_{\text{B.Z.}} d^2\mathbf{K} \{c_2^{(1)}(\mathbf{K}; H) - c_2^{(-1)}(\mathbf{K}; H)\} F_{xy}^{(1)}(\mathbf{K}; H), \quad (\text{B1})$$

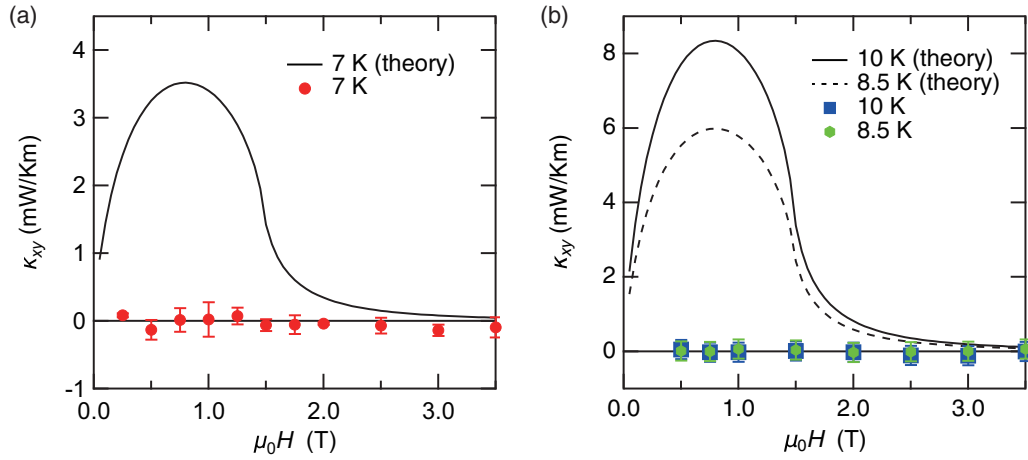


FIG. 9. (a) and (b) Comparison of experimental and theoretical thermal Hall conductivities. The magnitude of the observed κ_{xy} (symbols) is much smaller than that of the κ_{xy} calculated by the formula given in Ref. [34] (solid and dashed curves).

with l_z being the interlayer distance and the function $c_2(\rho)$ given by

$$\begin{aligned}
 c_2^{(m)}(\mathbf{K}; H) &\equiv c_2[\rho_B(\epsilon^{(m)}(\mathbf{K}; H))], \\
 c_2(\rho) &\equiv -2\text{Li}_2(-\rho) - \log^2(\rho) \\
 &\quad + (\rho + 1) \log^2\left(\frac{\rho + 1}{\rho}\right), \\
 \rho_B(\epsilon) &= \frac{1}{e^{\frac{\epsilon}{k_B T}} - 1}.
 \end{aligned} \tag{B2}$$

All the information about the thermally excited triplons is encoded in the factor $\{c_2^{(1)}(\mathbf{K}; H) - c_2^{(-1)}(\mathbf{K}; H)\}$. We note that, compared with the value of κ_{xy} in the previous studies [30,34], the one given by Eq. (B1) is opposite in sign and smaller in magnitude by $(2\pi)^{-1}$. While our main conclusion remains unchanged even if we used the values calculated by the formula in Ref. [34] that further suppress the ratio $\kappa_{xy}^{(\text{exp})}/\kappa_{xy}^{(\text{th})}$ between the experimental and theoretical values by a factor $(2\pi)^{-1}$ (see Fig. 9), it is desirable to reexamine the previous theoretical calculations.

A few remarks are in order here about the relation between the topology of the triplon bands and the thermal Hall transport. First of all, in contrast to the electrical counterpart in fermion systems, the thermal Hall response of the triplon quasiparticles is *not* quantized to the Chern number $\mathcal{C}^{(m)}$ (up to a constant of proportionality) although finite Berry curvature $F_{xy}^{(m)}(K_x, K_y)$ suggests finite thermal Hall transport [5,6]. Moreover, the existing formula connecting the Berry curvature $F_{xy}^{(m)}(K_x, K_y)$ and the thermal Hall conductivity is derived by assuming the existence of the stable quasiparticles that can be treated as noninteracting. As will be discussed later, the geometrically suppressed kinetic energy of triplons in $\text{SrCu}_2(\text{BO}_3)_2$ prevents their spontaneous decay at $T = 0$ [15,37] that may potentially invalidate the picture based on topologically nontrivial quasiparticles. Therefore this system seems to provide a unique playground to study the topological properties of bosonic quasiparticles.

2. Effects of interlayer interactions

As has been discussed in Sec. IV B, only the interlayer DM interactions can crucially affect the thermal Hall conductivity. Symmetry analyses tell us that the possible interlayer DM interactions (on the shortest bonds connecting the upper and lower layers) are of the following form (see Fig. 4):

$$\begin{aligned}
 \mathbf{d}_1 &= (-d_y, -d_y, d_z), & \mathbf{d}_2 &= (-d_y, d_y, -d_z), \\
 \mathbf{d}_3 &= (d_y, -d_y, -d_z), & \mathbf{d}_4 &= (d_y, d_y, d_z), \\
 \mathbf{d}'_1 &= (-d'_y, -d'_y, d'_z), & \mathbf{d}'_2 &= (-d'_y, d'_y, -d'_z), \\
 \mathbf{d}'_3 &= (d'_y, -d'_y, -d'_z), & \mathbf{d}'_4 &= (d'_y, d'_y, d'_z),
 \end{aligned} \tag{B3}$$

with $d_{y,z}$ and $d'_{y,z}$ remaining undetermined solely by symmetry. Due to the buckling in the CuBO_3 (*ab*) planes, $d_{y,z}$ and $d'_{y,z}$ are different, in general. The alternate stacking of the Shastry-Sutherland layers in the *c* direction implies a period-2 structure in the stacking direction, and the unit cell now contains four dimers [(A1, B1) for the first layer and (A2, B2) for the second]. Correspondingly, the single-triplon hopping is now described by a 12×12 matrix.

For the interlayer DM interactions shown in Fig. 4 and Eq. (B3), the interlayer part of the triplon Hamiltonian is given by

$$\begin{aligned}
 \mathcal{H}_{\text{interlayer}}(\mathbf{k}) &= \begin{pmatrix} \mathbf{0}_{3 \times 3} & \mathbf{0}_{3 \times 3} & \mathbf{0}_{3 \times 3} & M_{A1B2}(\mathbf{k}) \\ \mathbf{0}_{3 \times 3} & \mathbf{0}_{3 \times 3} & M_{A2B1}^\dagger(\mathbf{k}) & \mathbf{0}_{3 \times 3} \\ \mathbf{0}_{3 \times 3} & M_{A2B1}(\mathbf{k}) & \mathbf{0}_{3 \times 3} & \mathbf{0}_{3 \times 3} \\ M_{A1B2}^\dagger(\mathbf{k}) & \mathbf{0}_{3 \times 3} & \mathbf{0}_{3 \times 3} & \mathbf{0}_{3 \times 3} \end{pmatrix}
 \end{aligned} \tag{B4}$$

and

$$\begin{aligned}
 M_{A1B2}(\mathbf{k}) &\equiv e^{-i(k_x+k_y+k_z)} M_{AB}^\perp(d_z) + e^{-i(k_x+k_y)} M_{AB}^\perp(d'_z) \\
 &= e^{-i(k_x+k_y+k_z)} (d_z + d'_z e^{ik_z}) \begin{pmatrix} 0 & 1 & 0 \\ -1 & 0 & 0 \\ 0 & 0 & 0 \end{pmatrix}, \\
 M_{A2B1}(\mathbf{k}) &\equiv M_{AB}^\perp(d_z) + e^{ik_z} M_{AB}^\perp(d'_z) \\
 &= e^{i(k_x+k_y+k_z)} M_{A1B2}(\mathbf{k})
 \end{aligned} \tag{B5}$$

(note that the momentum \mathbf{k} here is defined with respect to the original lattice and is different from \mathbf{K}).

Although no quantitative information is available now for the values of $d_{y,z}$ and $d'_{y,z}$ in $\text{SrCu}_2(\text{BO}_3)_2$, we can obtain a very crude estimate by comparing the energy levels at the Γ point with the ESR spectrum. Figure 6 plots the 12 energy levels for several values of the interlayer DM interaction d_z , where one can clearly see that finite values of d_z further split the six energy levels found for $d_z = 0$. No such splitting has been observed in ESR measurements (see Fig. 4(a) of Ref. [33]), and we may conclude that the interlayer DM interactions are, if they exist, much smaller than those within each plane (i.e., D'_\parallel and D'_\perp).

For the sake of the simplicity, let us assume $d_z = d'_z$, which allows us to work with a smaller unit cell (now two species of dimers A and B are identified) and express the interlayer hopping matrix by the following three-dimensional matrix:

$$\mathcal{H}_{\text{interlayer}}(\mathbf{K}) = \begin{pmatrix} 0 & 2id_z \cos K_z & 0 \\ -2id_z \cos K_z & 0 & 0 \\ 0 & 0 & 0 \end{pmatrix}. \quad (\text{B6})$$

Comparing this with the 2D Hamiltonian equation (A2), one sees that the net effect of the interlayer DM interactions is just to shift the external field in a K_z -dependent way:

$$H \rightarrow H^{\text{eff}}(K_z) = H + \frac{2d_z}{g_z \mu_B} \cos K_z l_z, \quad (\text{B7})$$

and the summation over different layers is replaced with the K_z integral. In the above expression, we have recovered the interlayer distance l_z for later convenience. As we have the same three-level Hamiltonian (A2) with $H \rightarrow H^{\text{eff}}(K_z)$, the Berry curvature in the (K_x, K_y) plane for a given K_z is readily obtained just by replacing H in Eq. (A5) with $H^{\text{eff}}(K_z)$.

Now it is straightforward to write down κ_{xy} for a 3D stack of the Shastry-Sutherland layers by trading \sum_{layer} in Eq. (B1) for the summation over K_z :

$$\begin{aligned} \kappa_{xy}^{\text{3D}}(T, H_z) &= -\frac{k_B^2 T}{\hbar L_x L_y L_z} \sum_{m=-1,0,+1} \sum_{K_z} \\ &\times \sum_{\mathbf{K}=(K_x, K_y)} \tilde{c}_2^{(m)}(\mathbf{K}; K_z) F_{xy}^{(m)}(\mathbf{K}; K_z) \\ &= -\frac{k_B^2 T}{\hbar L_x L_y L_z} \frac{L_x L_y L_z}{(2\pi)^3} \int_{-\pi/l_z}^{\pi/l_z} dK_z \\ &\times \int_{\text{B.Z.}} d^2 \mathbf{K} \{ \tilde{c}_2^{(1)}(\mathbf{K}; K_z) \\ &- \tilde{c}_2^{(-1)}(\mathbf{K}; K_z) \} F_{xy}^{(1)}(\mathbf{K}; K_z) \\ &= \frac{l_z}{2\pi} \int_{-\pi/l_z}^{\pi/l_z} dK_z \kappa_{xy}(T, H; K_z), \end{aligned} \quad (\text{B8})$$

where

$$\begin{aligned} \tilde{c}_2^{(m)}(\mathbf{K}; K_z) &= c_2^{(m)}(\mathbf{K}; H = H_{\text{eff}}(K_z)), \\ \kappa_{xy}(T, H; K_z) &= \kappa_{xy}(T, H = H_{\text{eff}}(K_z)). \end{aligned} \quad (\text{B9})$$

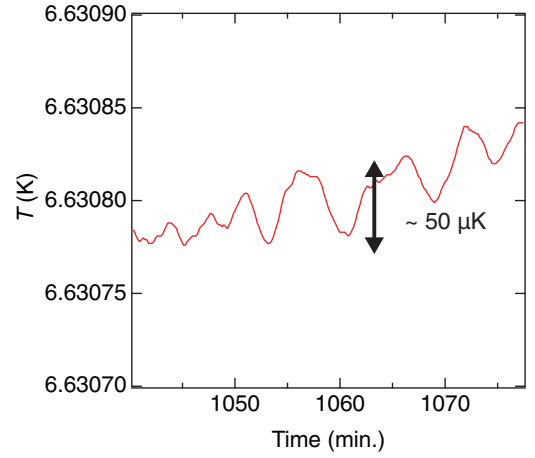


FIG. 10. Precise control of temperature during thermal Hall conductivity κ_{xy} measurements.

When $d_z = 0$, $\kappa_{xy}(T, H; K_z)$ does not depend on K_z , and the above $\kappa_{xy}^{\text{3D}}(T, H_z)$ reduces to $\kappa_{xy}(T, H_z)$ in Eq. (B1).

In order to further simplify the expression, we trade the K_z integral with the integral over the effective field,

$$h_z \equiv H + \frac{2d_z}{g_z \mu_B} \cos K_z l_z \quad \left(H - \frac{2|d_z|}{g_z \mu_B} \leq h_z \leq H + \frac{2|d_z|}{g_z \mu_B} \right),$$

to obtain the final expression (2):

$$\kappa_{xy}^{\text{3D}}(T, H) = \frac{1}{\pi} \int_{H - \frac{2|d_z|}{g_z \mu_B}}^{H + \frac{2|d_z|}{g_z \mu_B}} dh_z \frac{\kappa_{xy}(T, h_z)}{\sqrt{\left(\frac{2d_z}{g_z \mu_B}\right)^2 - (h_z - H)^2}}. \quad (\text{B10})$$

The values obtained using this formula are shown in Fig. 5.

APPENDIX C: HIGH-RESOLUTION MEASUREMENTS OF THERMAL HALL CONDUCTIVITY

A typical temperature noise level δT is $\sim 50 \mu\text{K}$ at $T \sim 7 \text{K}$ ($\delta T/T \sim 10^{-5}$) (see Fig. 10), which enables us to achieve high-precision measurements of κ_{xy} . In addition, we repeated the κ_{xy} measurements more than 10 times at 0.75 and 1 T

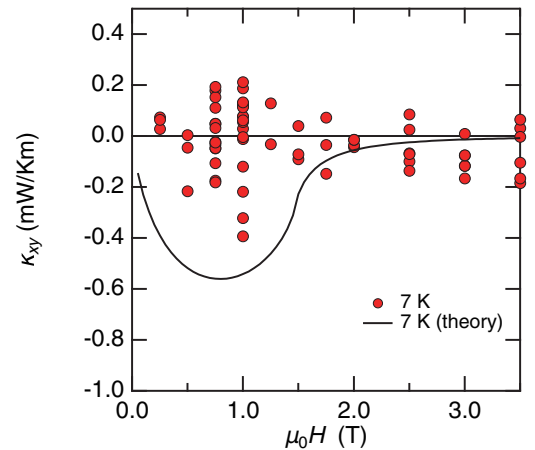


FIG. 11. Statistical error of κ_{xy} . The error bars in Fig. 3(a) in the main text indicate the standard statistical errors obtained from multiple measurements (red circles).

(see Fig. 11), where considerable κ_{xy} of $\sim 0.5 \text{ mW K}^{-1} \text{ m}^{-1}$ is expected. This allows us to quantitatively compare the experi-

mental results with the theoretical calculations (black curve in Fig. 11).

-
- [1] L. Zhang, J. Ren, J.-S. Wang, and B. Li, *Phys. Rev. B* **87**, 144101 (2013).
- [2] A. Mook, J. Henk, and I. Mertig, *Phys. Rev. B* **89**, 134409 (2014).
- [3] R. Chisnell, J. S. Helton, D. E. Freedman, D. K. Singh, R. I. Bewley, D. G. Nocera, and Y. S. Lee, *Phys. Rev. Lett.* **115**, 147201 (2015).
- [4] P. A. McClarty, *Annu. Rev. Condens. Matter Phys.* **13**, 171 (2022).
- [5] H. Katsura, N. Nagaosa, and P. A. Lee, *Phys. Rev. Lett.* **104**, 066403 (2010).
- [6] R. Matsumoto and S. Murakami, *Phys. Rev. Lett.* **106**, 197202 (2011).
- [7] Y. Onose, T. Ideue, H. Katsura, Y. Shiomi, N. Nagaosa, and Y. Tokura, *Science* **329**, 297 (2010).
- [8] T. Ideue, Y. Onose, H. Katsura, Y. Shiomi, S. Ishiwata, N. Nagaosa, and Y. Tokura, *Phys. Rev. B* **85**, 134411 (2012).
- [9] M. Hirschberger, J. W. Krizan, R. Cava, and N. Ong, *Science* **348**, 106 (2015).
- [10] M. Hirschberger, R. Chisnell, Y. S. Lee, and N. P. Ong, *Phys. Rev. Lett.* **115**, 106603 (2015).
- [11] D. Watanabe, K. Sugii, M. Shimozawa, Y. Suzuki, T. Yajima, H. Ishikawa, Z. Hiroi, T. Shibauchi, Y. Matsuda, and M. Yamashita, *Proc. Natl. Acad. Sci. USA* **113**, 8653 (2016).
- [12] H. Doki, M. Akazawa, H.-Y. Lee, J. H. Han, K. Sugii, M. Shimozawa, N. Kawashima, M. Oda, H. Yoshida, and M. Yamashita, *Phys. Rev. Lett.* **121**, 097203 (2018).
- [13] M. Akazawa, M. Shimozawa, S. Kittaka, T. Sakakibara, R. Okuma, Z. Hiroi, H.-Y. Lee, N. Kawashima, J. H. Han, and M. Yamashita, *Phys. Rev. X* **10**, 041059 (2020).
- [14] Z.-X. Li, Y. Cao, and P. Yan, *Phys. Rep.* **915**, 1 (2021).
- [15] A. L. Chernyshev and P. A. Maksimov, *Phys. Rev. Lett.* **117**, 187203 (2016).
- [16] C. Strohm, G. L. J. A. Rikken, and P. Wyder, *Phys. Rev. Lett.* **95**, 155901 (2005).
- [17] K. Sugii, M. Shimozawa, D. Watanabe, Y. Suzuki, M. Halim, M. Kimata, Y. Matsumoto, S. Nakatsuji, and M. Yamashita, *Phys. Rev. Lett.* **118**, 145902 (2017).
- [18] T. Ideue, T. Kurumaji, S. Ishiwata, and Y. Tokura, *Nat. Mater.* **16**, 797 (2017).
- [19] H. J. Xiang, E. J. Kan, M.-H. Whangbo, C. Lee, S.-H. Wei, and X. G. Gong, *Phys. Rev. B* **83**, 174402 (2011).
- [20] K. Riedl, D. Guterding, H. O. Jeschke, M. J. P. Gingras, and R. Valentí, *Phys. Rev. B* **94**, 014410 (2016).
- [21] H. Kageyama, K. Yoshimura, R. Stern, N. V. Mushnikov, K. Onizuka, M. Kato, K. Kosuge, C. P. Slichter, T. Goto, and Y. Ueda, *Phys. Rev. Lett.* **82**, 3168 (1999).
- [22] B. S. Shastry and B. Sutherland, *Physica B (Amsterdam)* **108**, 1069 (1981).
- [23] P. Corboz and F. Mila, *Phys. Rev. B* **87**, 115144 (2013).
- [24] S. Miyahara and K. Ueda, *J. Phys.: Condens. Matter* **15**, R327(R) (2003).
- [25] H. Kageyama, M. Nishi, N. Aso, K. Onizuka, T. Yoshida, K. Nukui, K. Kodama, K. Kakurai, and Y. Ueda, *Phys. Rev. Lett.* **84**, 5876 (2000).
- [26] S. Miyahara and K. Ueda, *Phys. Rev. Lett.* **82**, 3701 (1999).
- [27] M. Takigawa, T. Waki, M. Horvatić, and C. Berthier, *J. Phys. Soc. Jpn.* **79**, 011005 (2010).
- [28] Y. F. Cheng, O. Cépas, P. W. Leung, and T. Ziman, *Phys. Rev. B* **75**, 144422 (2007).
- [29] J. Romhányi, K. Totsuka, and K. Penc, *Phys. Rev. B* **83**, 024413 (2011).
- [30] P. A. McClarty, F. Krüger, T. Guidi, S. Parker, K. Refson, A. Parker, D. Prabhakaran, and R. Coldea, *Nat. Phys.* **13**, 736 (2017).
- [31] B. D. Gaulin, S. H. Lee, S. Haravifard, J. P. Castellán, A. J. Berlinsky, H. A. Dabkowska, Y. Qiu, and J. R. D. Copley, *Phys. Rev. Lett.* **93**, 267202 (2004).
- [32] M. E. Zayed, C. Rüegg, T. Strässle, U. Stühr, B. Roessli, M. Ay, J. Mesot, P. Link, E. Pomjakushina, M. Stingaciu, K. Conder, and H. M. Rønnow, *Phys. Rev. Lett.* **113**, 067201 (2014).
- [33] H. Nojiri, H. Kageyama, Y. Ueda, and M. Motokawa, *J. Phys. Soc. Jpn.* **72**, 3243 (2003).
- [34] J. Romhányi, K. Penc, and R. Ganesh, *Nat. Commun.* **6**, 6805 (2015).
- [35] M. Malki and K. P. Schmidt, *Phys. Rev. B* **95**, 195137 (2017).
- [36] H. Sun, P. Sengupta, D. Nam, and B. Yang, *Phys. Rev. B* **103**, L140404 (2021).
- [37] M. E. Zhitomirsky and A. L. Chernyshev, *Rev. Mod. Phys.* **85**, 219 (2013).
- [38] M. Hofmann, T. Lorenz, G. S. Uhrig, H. Kierspel, O. Zabara, A. Freimuth, H. Kageyama, and Y. Ueda, *Phys. Rev. Lett.* **87**, 047202 (2001).
- [39] We found a factor $1/(2\pi)$ missing in the formula given in Ref. [34], which had been probably overlooked in recovering the physical constants (\hbar , k_B , etc.) in the formula equation (35) of the Supplementary Notes. We used the corrected formula (B1) for the theoretical values.
- [40] At this level of approximation, a small shift of the interdimer exchange J' just modifies the value of the spin gap J slightly, which may be absorbed into a small change of the temperature T . By directly evaluating (B1), we found that small changes in the DM interactions mainly shift the band-touching field but do not reduce κ_{xy} significantly.
- [41] L. P. Cairns, J.-P. Reid, R. Perry, D. Prabhakaran, and A. Huxley, in *Proceedings of the International Conference on Strongly Correlated Electron Systems (SCES2019)*, JPS Conference Proceedings (Physical Society of Japan, Tokyo, 2020), Vol. 30, p. 011089.
- [42] Precisely, these quantities depend on its effective value.
- [43] If we take into account the on-dimer DM interaction D , $\mathbf{T}_{A,B}$ contain the order D terms of the form $(\tilde{s}_{A,B}^\dagger \tilde{t}_{A,B,a} + \tilde{t}_{A,B,a}^\dagger \tilde{s}_{A,B})$, and J_\perp can generate interlayer triplon hopping processes (between A and B dimers) proportional to $D^2 J_\perp / J^2$. As these processes are much smaller than the interlayer hopping due to

- the interlayer DM interactions, we may neglect them at this level of approximation.
- [44] D. Bhowmick and P. Sengupta, *Phys. Rev. B* **104**, 085121 (2021).
- [45] K. Totsuka, S. Miyahara, and K. Ueda, *Phys. Rev. Lett.* **86**, 520 (2001).
- [46] Here, the momentum (K_x, K_y) is defined with respect to an effective square lattice obtained by neglecting the difference between the A and B dimers. It has a Brillouin zone twice larger than that of the original Shastry-Sutherland lattice.
- [47] S. Murakami and A. Okamoto, *J. Phys. Soc. Jpn.* **86**, 011010 (2016).